Modulation of In Vivo Alloreactivity by Inhibition of Inducible Nitric Oxide Synthase

By Neil K. Worrall,* W. Douglas Lazenby,* Thomas P. Misko,§ Tien-Sung Lin,¶ Charles P. Rodi,‖ Pamela T. Manning,§ Ronald G. Tilton,‡ Joseph R. Williamson,‡ and T. Bruce Ferguson, Jr.*

*From the Departments of *Surgery (Division of Cardiothoracic Surgery) and ‡Pathology, Washington University School of Medicine, Saint Louis, Missouri 63110; the Departments of §Molecular Pharmacology and ‖Cellular and Molecular Biology, Searle Research and Development, Monsanto Company, Saint Louis, Missouri 63167; and the ¶Department of Chemistry, Washington University, Saint Louis, Missouri 63130*

Summary

The role of nitric oxide in the immune response to allogeneic tissue was explored in an in vivo cardiac transplant model in the rat. Nitric oxide production during organ rejection was demonstrated by elevations in systemic serum nitrite/nitrate levels and by electron paramagnetic resonance spectroscopy. Messenger RNA for the inducible nitric oxide synthase enzyme was detected in the rejecting allografted heart, but not in the nonrejecting isografted heart. The enzyme was demonstrated to be biologically active by the in vitro conversion of L-arginine to L-citrulline and was immunohistochemically localized to the infiltrating inflammatory cells. Treatment with aminoguanidine, a preferential inhibitor of the inducible nitric oxide synthase isoform, prevented the increased nitric oxide production in the transplanted organ and significantly attenuated the pathogenesis of acute rejection. Aminoguanidine treatment prolonged graft survival, improved graft contractile function, and significantly reduced the histologic grade of rejection. These results suggest an important role for nitric oxide in mediating the immune response to allogeneic tissue. Inhibition of inducible nitric oxide synthase may provide a novel therapeutic modality in the management of acute transplant rejection and of other immune-mediated processes.

Acute rejection is mediated by humoral and cellular immune mechanisms, and is characterized by an intense inflammatory cell infiltrate and progressive destruction of the grafted organ. Despite many recent advances in the understanding of the immune system, the regulatory and effector mechanisms underlying the rejection process remain incompletely understood. Recent reports have demonstrated production of the free radical nitric oxide (NO)[1] during organ transplant rejection (1, 2). NO is synthesized from the amino acid L-arginine by a family of enzymes, the nitric oxide synthases (NOS), and is involved in diverse physiologic and pathophysiologic processes, including host immune defense, vasoregulation, neurotransmission, and diabetes (3, 4).

In addition to its role as a cellular messenger at low concentrations, NO is thought to be involved in pathologic processes because of its cytotoxicity at high concentrations. The inducible form of NOS (iNOS) produces large amounts of NO, can be expressed in diverse cell types, and in part mediates the cytostatic and cytotoxic effector function of activated macrophages (5, 6). Aminoguanidine is a selective iNOS inhibitor (7) that recently has been demonstrated to attenuate the pathophysiologic sequelae of NO production in diabetes (8, 9), uveitis (10), and in experimental autoimmune encephalomyelitis (11). Despite the detection of NO during the rejection process and the demonstration of the in vitro immunoregulatory properties of NO (12–15), the role of NO in the in vivo immune response to allogeneic tissue is unclear. This report demonstrates that NO is pro-

[1] *Abbreviations used in this paper:* EPR, electron paramagnetic resonance; iNOS, inducible nitric oxide synthase; NO, nitric oxide; NOS, nitric oxide synthase; POD, postoperative day; RT-PCR, reverse transcriptase PCR.

Portions of this work were presented at the 30th Annual Meeting of the Society of Thoracic Surgeons, New Orleans, LA 31 January–2 February 1994.

J. Exp. Med. © The Rockefeller University Press • 0022-1007/95/01/0063/08 $2.00
Volume 181 January 1995 63–70

duced during organ transplant rejection by the induction of iNOS in the inflammatory cells infiltrating the rejecting organ, and that inhibition of iNOS with aminoguanidine significantly ameliorated the pathogenesis of acute rejection.

Materials and Methods

Heterotopic Rat Cardiac Transplant Model. Male 175–200 g Lewis (RT-1^l major histocompatibility antigen haplotype) and ACI (RT-1^a) rats were purchased from Harlan-Sprague-Dawley (Indianapolis, IN). The animals received standard rat chow and water ad libitum and were housed and cared for in accordance with guidelines set forth by the Washington University Committee for the Humane Care of Laboratory Animals and the National Institutes of Health regarding laboratory animal welfare. Allogeneic (Lewis donor to ACI recipient) and syngeneic (ACI to ACI) heterotopic intra-abdominal cardiac transplantation was performed essentially as described (16). The grafted hearts were monitored by daily palpation and complete rejection was defined as the cessation of palpable contractile activity.

Spectrofluorometric Determination of Serum Nitrite/Nitrate. Systemic serum nitrite/nitrate levels were measured in blood samples taken from the thoracic inferior vena cava at the time of animal sacrifice. Red blood cells were removed by centrifugation and the resulting serum filtered through an Ultrafree-MC microcentrifuge filter (Millipore Corp.; Bedford, MA) to remove the hemoglobin resulting from cell lysis. After conversion of nitrate to nitrite with nitrate reductase (Sigma Chemical Co., St. Louis, MO), total nitrite was measured by reacting with 2,3-diaminonaphthalene (Aldrich Chemical Co., Milwaukee, WI) under acidic conditions to form 1-(*H*)-naphthotriazole, a fluorescent product, as described (17). The formation of 1-(*H*)-naphthotriazole was quantitated using a fluorescent plate reader (Pandex; IDEXX Laboratories, Inc., Westbrook, ME) with excitation at 365 nm and emission read at 450 nm.

Reverse Transcriptase (RT) PCR. Transplanted hearts were harvested by rapid excision and flash frozen in liquid nitrogen. Total RNA was extracted using guanidinium thiocyanate as described (18). First strand cDNA was prepared from 1 μg of RNA using Superscript™ II RNase H^- Reverse Transcriptase (GIBCO-BRL, Gaithersburg, MD) under the conditions suggested by the supplier. Using a Roche Molecular Systems kit (Branchburg, NJ) with 1.5 mM $MgCl_2$, PCR was performed with primers specific for iNOS (TAGAAACAACAGGAACCTACCA and ACAGGGGTGATGCTCCCGGACA), yielding a 907-bp product; and for glyceraldehyde-3-phosphate dehydrogenase ([G3PDH]; GACTCGAATTCTACCCACGGCAAGTTCAATGG and GACTCGAATTCAGGGGCGGAGATGATGACCC) to yield a 224-bp product. Cycle times were 1 min at 95°C, 1 min at 60°C, and 1 min at 72°C for 30 cycles. 10% of the iNOS reaction was combined with 5% of the G3PDH reaction and analyzed for the presence or absence of the iNOS species by electrophoresis on a 1% agarose gel.

iNOS Activity. L-citrulline production was determined in allograft, isograft, and normal hearts as described (19; $n = 3$ for each group; all reagents from Sigma Chemical Co. unless otherwise indicated). The hearts were minced and homogenized with a Polytron homogenizer (Brinkmann Instruments, Inc., Westbury, NY) in 1.5 ml of deionized water containing 1 mM dithiothreitol (DTT), 1 μM tetrahydrobiopterin, 2 μM flavin adenine dinucleotide (FAD), 10 μg/ml pepstatin, 10 μg/ml antipain, 10 μg/ml soybean trypsin inhibitor, 10 μM leupeptin, 10 μM chymostatin, and 0.5 mM PMSF. Each homogenate was then supplemented with 10% glycerol. NOS activity was measured by monitoring the conversion of L-[2,3-^{3}H]arginine (DuPont-NEN, Boston, MA) to L-[2,3-^{3}H]citrulline (19). 50-μl samples were run in duplicate in the presence or absence of 1 mM N^G-monomethyl-L-arginine (L-NMA). To initiate the reaction, an equal volume of 50 mM Tris, pH 7.6, containing the following components, was added: 2 mg/ml BSA, 5 mM EGTA (to block calcium-dependent constitutive NOS activity), 2 mM DTT, 20 μM FAD, 100 μM tetrahydrobiopterin, 2 mM NADPH, and 60 μM L-arginine containing 0.9 μCi of L-[2,3-^{3}H]-arginine. After incubation at 37°C for 40 min, the reaction was terminated by addition of 300 μl cold stop buffer containing 10 mM EGTA, 100 mM Hepes, pH 5.5, and 1 mM L-citrulline. The [^{3}H]citrulline was separated by chromatography on Dowex 50W X-8 cation exchange resin (Sigma Chemical Co.) and radioactivity quantified with a liquid scintillation counter.

Immunohistochemistry. Immunohistochemical staining of iNOS was performed using 10 μm frozen sections of the allograft heart, isograft heart, and normal ACI rat heart ($n = 3$ for each group). Tissues were fixed with 1% paraformaldehyde, pH 7.2, for 5 min at room temperature, followed by 100% ethanol for 5 min at 4°C. Nonspecific binding was blocked with 3% normal goat serum in 0.5 M Tris-HCl, pH 7.4, for 1 h at room temperature. All subsequent incubations were carried out in this buffer. Tissue sections were incubated with 1:1,000 dilution of either preimmune rabbit sera or an anti-iNOS antisera generated in rabbits to a unique peptide sequence obtained from the COOH-terminal region of murine iNOS (AVFSYGAKKGSALEEPKATRL) for 16 h at 4°C. Endogenous peroxidase activity was reduced with periodic acid (Zymed Laboratories, Inc., S. San Francisco, CA) for 45 s at room temperature, followed by sequential incubations with biotinylated anti-rabbit IgG and avidin-biotin-peroxidase complex (Vector Laboratories, Inc., Burlingame, CA) for 2 h each. The reaction product was visualized using 3,3′-diaminobenzidine intensified with nickel chloride for 6 min. Tissue sections were counterstained with Mayer's hematoxylin and mounted.

Aminoguanidine Administration. Aminoguanidine-treated allografts received continuous intravenous infusion of aminoguanidine hemisulfate (Sigma Chemical Co.) in 0.9% NaCl (600 $mg \cdot kg^{-1} \cdot d^{-1}$) via a right external jugular vein cannula connected to a subcutaneously implanted osmotic infusion pump (Alza Corp., Palo Alto, CA) from the time of transplantation until harvest on postoperative day 8 (POD-8) for histologic and electron paramagnetic resonance spectroscopy (EPR) analysis or until complete rejection occurred. Control allografts received continuous IV infusion of 0.9% NaCl from a similarly implanted pump. For the papillary muscle experiments, aminoguanidine-treated allografts received 100 mg/kg of aminoguanidine subcutaneously every 6 h beginning at the time of transplantation (total dose of 400 $mg \cdot kg^{-1} \cdot d^{-1}$) until harvest on POD-4. Control allograft and isograft rats received 0.9% NaCl subcutaneously in a similar fashion.

Contractile Function of the Grafted Heart. Isolated right ventricular papillary muscle function was determined essentially as described (20). Briefly, the native or the grafted heart was explanted into oxygenated modified Tryode's solution which had the following composition ([mM] 5.0 K^+, 140.0 Na^+, 0.5 Ca^{2+}, 28.0 HCO_3^-, 1.2 PO_4^{2-}, 1.2 Mg^{2+}, 1.2 SO_4^{2-}, and 5 glucose) and a right ventricular papillary muscle excised, mounted in a tissue perfusion bath attached to a calibrated force transducer (model FT03; Grass Instruments, Quincy MA), and superfused with the same solution equilibrated with 95% O_2/5% CO_2 to a final pH of 7.4 at 31°C. The muscles were field stimulated with platinum electrodes (0.3 Hz, 6-millisecond duration) at two times the pacing threshold. After an initial recovery period of 30 min, the muscles were loaded to the length of maximal activation and equilibrated for 90 min,

and then challenged by increasing the [Ca^{2+}] to 2.0 mM. The tension developed during isometric contraction was continuously recorded on an analog chart recorder (RS 3400; Gould Electronics, Cleveland, OH). The maximal tension developed at each [Ca^{2+}] was normalized to the mean cross-sectional area and reported as millinewtons/mm^3.

EPR. EPR was performed on the allografted heart on POD-4 (n = 4), POD-5 (n = 4), POD-8 (n = 7); on the allograft native heart on POD-8 (n = 4); on the aminoguanidine-treated allograft heart on POD-8 (n = 7); and on the isografted heart on POD-8 (n = 4). At the time of tissue harvest, the left ventricular apex (~100 mg) was amputated, placed into a 4-mm quartz EPR tube (Wilmad Glass, Buena, NJ), flash frozen in liquid nitrogen, and stored at −70°C until analyzed (in triplicate) at 30°K on an X-band spectrometer (model ER200; Bruker, Billerica, MA) equipped with an EPR cryostat (4.2-300 K; Oxford Scientific, Concord, MA). Signal averaging and data processing were implemented by an additional 12-bit analog/digital converter and a Scientific EPR software package (Scientific Software Services, Bloomington, IL). Experimental settings were: microwave frequency, 9.47 GHz; modulation frequency, 100 KHz; modulation amplitude, 5G; receiver gain, 2.5 × 10^4; and microwave power, 1.3 mW. The stable radical, 1,1-diphenyl-2-picrylhydrazyl was used as a field marker (g = 2.0036).

Histology. The grafted heart was rapidly excised, fixed in 10% neutral buffered formaldehyde, embedded in paraffin, cross-sectioned, stained with hematoxylin and eosin, and then graded for acute rejection using a modification of the Billingham criteria (21). In a blinded fashion, four separate sections from each specimen were graded for both interstitial infiltrate and myocyte necrosis: 0 = no infiltrate or necrosis; 1 = mild, scattered mononuclear infiltrate or rare necrosis; 2 = moderate infiltrate or patchy necrosis; 3 = moderately severe infiltrate or necrosis; 4 = severe infiltrate or necrosis; and 5 = complete rejection.

Statistical Analysis. Papillary muscle contractile function data and serum nitrite/nitrate measurements were analyzed by analysis of variance (ANOVA) with the Tukey HSD posthoc test for multiple comparisons; histologic grading scores were compared by Student's unpaired t-test; and graft survival data were compared by Kaplan-Meier analysis with the Mantel-Haenszel log rank test using SYSTAT (SYSTAT Inc., Evanston, IL). Data are expressed as mean ± SEM unless otherwise indicated, with a $p < 0.05$ considered statistically significant.

Results and Discussion

The time course of NO production during cardiac allograft rejection was determined by measuring the systemic serum nitrite/nitrate levels at serial time points after transplantation (Fig. 1). Nitrite and nitrate are stable endproducts of NO metabolism and thus serve as indirect markers for the presence of NO (2). In this rat model, isograft serum nitrite/nitrate levels did not vary from normal control values (15 ± 1 μM; n = 6) throughout the postoperative course. Allograft serum nitrite/nitrate levels were first elevated above isograft and normal control values on POD-4, coinciding with the first histologically detectable evidence of acute rejection. The fall in systemic serum nitrite/nitrate levels measured in the latter stages of rejection likely reflect decreased release from the graft, possibly secondary to thrombosis and destruction of the graft microvasculature, rather than reduced NO production (see discussion of EPR results below). The two-

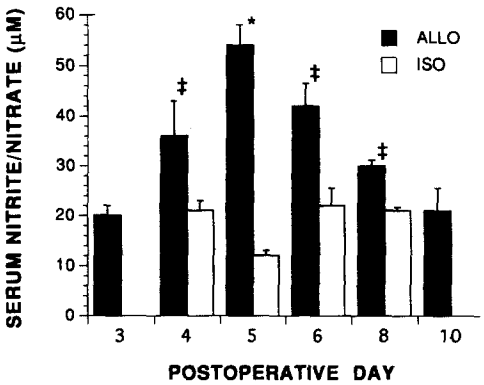

Figure 1. Serum nitrite/nitrate levels measured at serial time points after transplantation. Allograft (*ALLO*) and isograft (*ISO*) transplant recipients were harvested on the indicated day and serum nitrite/nitrate levels measured as described in Materials and Methods. Normal ACI control values were 15 ± 1 μM (n = 6). Mean ± SEM; n = 4–7; significant versus isograft at * = $p < 0.001$ and ‡ = $p < 0.05$.

to fourfold elevation in allograft systemic serum nitrite/nitrate levels suggested that iNOS, which is capable of sustained production of large quantities of NO, is induced during the rejection process.

Using RT-PCR amplification, the specific expression of iNOS mRNA during acute transplant rejection was demonstrated in the allograft heart on POD-5, but not in the isograft heart (Fig. 2). iNOS activity in the allograft myocardium was demonstrated by the calcium-independent conversion of L-arginine to L-citrulline by crude homogenates of cardiac allografts harvested on POD-5. L-citrulline production by the allografts was 40.4 ± 9.8 pmol and was over 80% inhibited by 1 mM L-NMA, a NOS inhibitor (7.1 ± 3.6 pmol). L-citrulline production could not be detected in isograft or normal hearts (0 ± 0 pmol).

Immunohistochemical staining of the allograft heart on POD-6 localized the iNOS to the infiltrating inflammatory cells (Fig. 3 *A*). The cells that stained for iNOS were principally clustered at sites of ongoing myocyte necrosis (Fig. 3 *B*). Although the inflammatory cell subtype cannot be precisely identified from these experiments, the cell morphology is suggestive of macrophages or lymphoblasts. iNOS was not

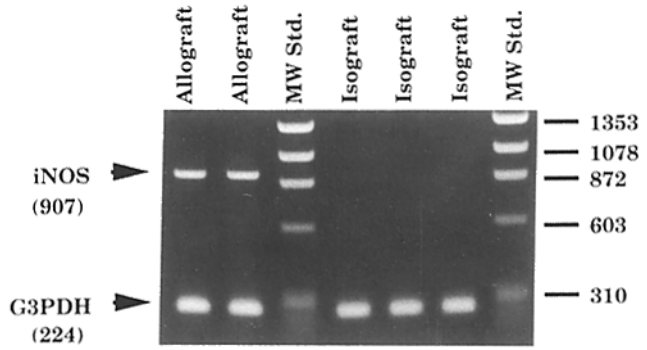

Figure 2. RT-PCR reaction detection of iNOS mRNA in the grafted heart on POD-5. iNOS mRNA is present in both allografts tested, but not in the three isografts tested.

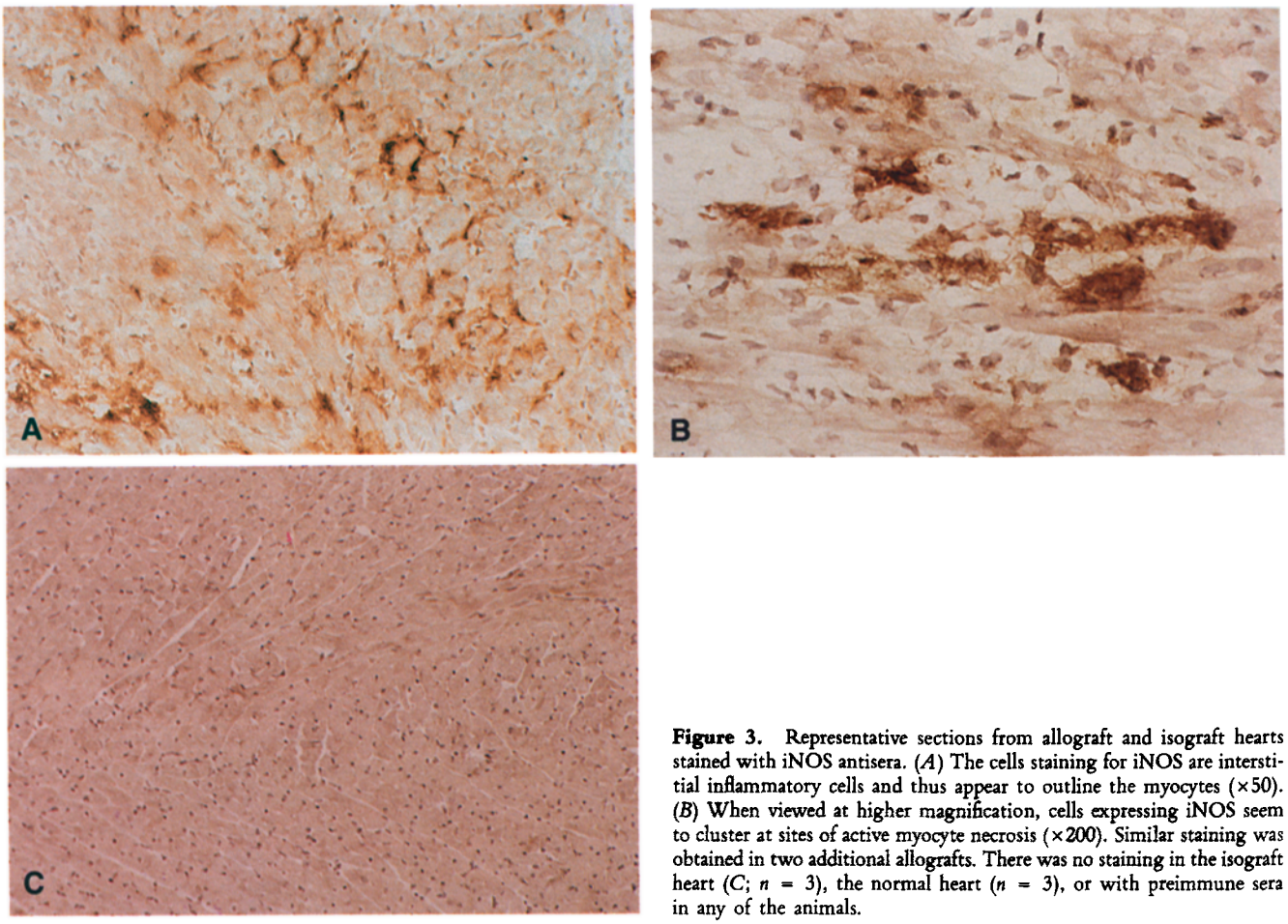

Figure 3. Representative sections from allograft and isograft hearts stained with iNOS antisera. (*A*) The cells staining for iNOS are interstitial inflammatory cells and thus appear to outline the myocytes (×50). (*B*) When viewed at higher magnification, cells expressing iNOS seem to cluster at sites of active myocyte necrosis (×200). Similar staining was obtained in two additional allografts. There was no staining in the isograft heart (*C*; $n = 3$), the normal heart ($n = 3$), or with preimmune sera in any of the animals.

present in isograft (Fig. 3 *C*) or normal rat hearts, and does not appear to be induced in the allograft endothelium, vascular smooth muscle, or myocytes. The RT-PCR, enzyme activity, and immunohistochemical data demonstrate that biologically active iNOS is expressed in the cells infiltrating the rejecting organ in a time frame consistent with a role in the rejection process.

To determine the contribution of iNOS to the pathogenesis of acute rejection, aminoguanidine, a selective iNOS inhibitor, was systemically administered to allograft recipients. Graft survival was significantly prolonged in all of the aminoguanidine-treated animals as compared to identical grafts in control animals (Table 1). The grafted hearts survived an average of 15.0 ± 1.53 d in the aminoguanidine-treated allografts and 10.14 ± 0.69 in the placebo-treated allograft controls. The prolongation of graft survival achieved with iNOS inhibition is like that obtained in a similar cardiac transplant model with low-dose cyclosporine A therapy or antibodies to tumor necrosis factor (22), suggesting an important role for NO in mediating the in vivo immune response to allogeneic tissue.

The effects of iNOS inhibition during in vivo rejection were further characterized by assessing the contractile function of the grafted heart. Papillary muscles isolated from aminoguanidine-treated allografts demonstrated significantly improved contractile function compared with untreated allografts and did not differ significantly from isograft papillary muscles (Fig. 4). Aminoguanidine treatment normalized the serum nitrite/nitrate levels measured at the time of graft

Table 1. *Inhibition of iNOS Prolongs Cardiac Allograft Survival*

Treatment group	Graft survival time	Graft survival time (mean ± SD)
	d	
Control	9, 10, 10, 10, 10, 11, 11	10.14 ± 0.69
Aminoguanidine	[13], 14, 15, 15, 15, 15, 18	15.0 ± 1.53*

Cardiac allograft recipients received treatment with either placebo or intravenous aminoguanidine from the time of transplantation until complete rejection. Graft survival was defined as the day after transplantation that palpable contractile activity ceased.

* Significant at $p < 0.001$; [ ], animal died with functioning graft and most likely reflects the 5% perioperative mortality rate with this model rather than the aminoguanidine treatment, as we have not observed mortality with aminoguanidine in normal rats.

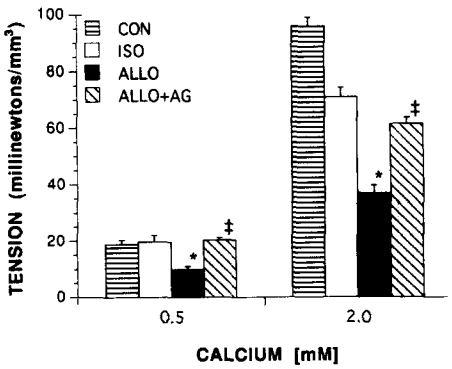

Figure 4. The contractile function of the grafted heart. Right ventricular papillary muscles were harvested on POD-4 from aminoguanidine-treated allograft (*ALLO + AG*), untreated allograft (*ALLO*), isograft (*ISO*), and normal Lewis (*CON*) hearts. Papillary muscle function was determined in response to a calcium challenge as described in Materials and Methods. ALLO-AG rats received 100 mg/kg of aminoguanidine subcutaneously every 6 h beginning at the time of transplantation. ALLO and ISO rats received 0.9% NaCl subcutaneously in a similar fashion. Mean ± SEM; $n = 6$; significant at $p < 0.005$ versus isograft (*) and untreated allograft (†), respectively.

harvest (19 ± 1 vs 36 ± 7 μM, $p < 0.05$; $n = 6$). Graft dysfunction during early cardiac rejection is thus mediated to a substantial degree by NO, and is therefore similar to cytokine-induced cardiac dysfunction, which is at least partially mediated by NO (20, 23).

EPR was used to examine the potential biochemical roles for NO in the pathogenesis of acute rejection. EPR analysis of the allograft myocardium demonstrated a specific NO signal (24) that was variably and weakly present on POD-4, uniformly present and of moderate intensity on POD-5, and that had reached maximal intensity by POD-8 (Fig. 5). Isograft heart and allograft native hearts did not demonstrate a signal for NO (Fig. 5). The strong EPR signal on POD-8 suggests that there is ongoing NO production in the latter stages of rejection. Thus, the fall in systemic serum nitrite/nitrate levels measured on POD-8 and -10 may reflect decreased release from the graft secondary to the immune-mediated destruction of the graft microvasculature, rather than reduced NO production. The EPR spectrum consists of a nitrogen hyperfine [(^{14}N); $I = 1$] with splitting of 17.5 gauss centered at $g = 2.011$ and an axial feature at $g = 2.040$, indicating the formation of nitrosylferromyoglobin and/or nitrosylferrohemoglobin and of nonheme iron–dinitrosyl complexes, respectively (1, 24–26). Nitrosylferromyoglobin and nitrosylferrohemoglobin are most likely formed because myoglobin and hemoglobin serve as biological sinks by spin trapping NO. The appearance of the nonheme iron–dinitrosyl complex signal in the allograft myocardium is consistent with NO-mediated cytostasis/cytotoxicity through the nitrosylation and inhibition of iron containing proteins such as mitochondrial electron transport chain complexes I and II, mitochondrial aconitase, and ribonucleotide reductase (5, 6, 25, 26).

Aminoguanidine treatment uniformly eliminated the EPR signals for nitrosylferromyoglobin, nitrosylferrohemoglobin, and for the nonheme iron–dinitrosyl complexes in the allografts

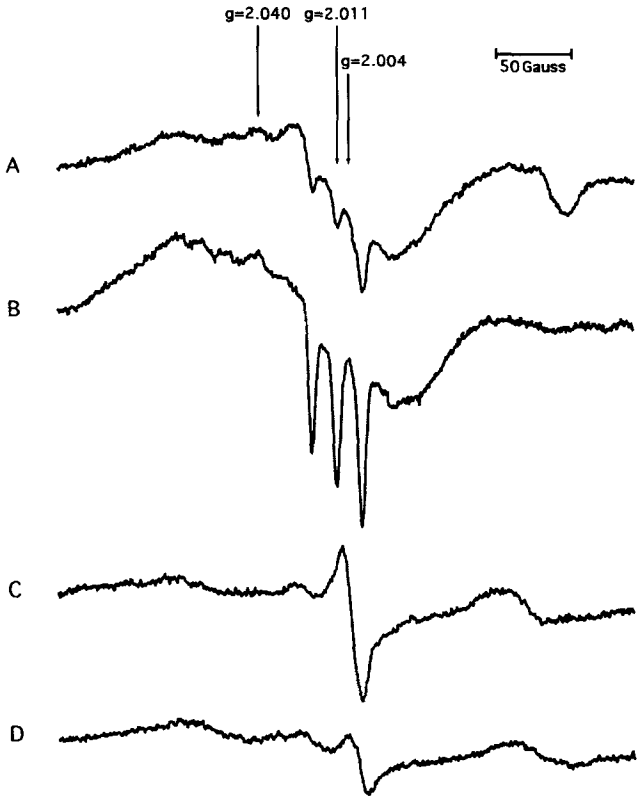

Figure 5. Representative EPR spectra of allograft and isograft hearts. The grafted heart was harvested from untreated allografts on POD-5 (*A*) and POD-8 (*B*); and on POD-8 from aminoguanidine-treated allografts (*C*) and untreated isografts (*D*). EPR was performed as described in Materials and Methods. $n = 4$–7 for each group.

(Fig. 5 *C* and Table 2). Eliminating the NO signal revealed a residual EPR signal ($g = 2.004$) that is different from the isograft signal (Fig. 5 *D*) and that is not an artifact of aminoguanidine treatment in that aminoguanidine-treated isografts demonstrate the same EPR signal as untreated isografts (our unpublished observations). The residual signal seen in aminoguanidine-treated allografts can be assigned to a semiquinone and/or a superoxide-free radical (27). Generation of these free radicals has not been previously demonstrated during organ rejection. In unmodified rejection, superoxide could combine with NO to form peroxynitrite and subsequently decompose to hydroxyl radical and nitrogen dioxide, which are much more toxic than NO itself (28). These breakdown products may be the actual effector molecules, and inhibition of iNOS could prevent their formation.

To determine the effect of iNOS inhibition at the tissue level, histologic analysis of the grafted heart was performed. Aminoguanidine treatment from the time of transplantation until harvest of the grafted heart on POD-8 normalized the serum nitrite/nitrate levels and significantly improved the histologic stage of rejection (Fig. 6 and Table 2). Control allografts demonstrated a dense interstitial inflammatory cell infiltrate and severe myocyte necrosis. Aminoguanidine-treated allografts were vigorously contracting at the time of harvest and demonstrated a significant reduction in myocardial necrosis. Perhaps

Table 2. *The Effect of iNOS Inhibition on NO Production and Histologic Rejection Grade*

Treatment group	EPR signal	Serum nitrite	Myocardial necrosis (0–5)	Interstitial infiltrate (0–5)
		(μM)		
Control (n = 7)	Present	30 ± 3	3.33 ± 0.52	3.50 ± 0.63
Aminoguanidine (n = 7)	Absent	11 ± 4*	1.64 ± 0.24‡	1.43 ± 0.35‡

Cardiac allograft recipients were treated with aminoguanidine or placebo from the time of transplantation until harvest on POD-8. The effect of iNOS inhibition on NO production and histologic rejection score were determined.
* Mean ± SD; significant versus control at p <0.001.
‡ Mean ± SD; significant versus control at p <0.0005.

even more striking is the decreased inflammatory cell infiltrate, suggesting a potential role for NO in the recruitment of inflammatory cells to the site of rejection.

These findings demonstrate that NO generated by the induction of iNOS in the inflammatory cell infiltrate modulates the in vivo immune response to allogeneic tissue. iNOS inhibition prevented the increased NO production in the transplanted organ and significantly attenuated the pathogenesis of acute rejection, as demonstrated by prolonged graft survival, improved graft contractile function, and a significant reduction in the histologic severity of rejection. NO may play both regulatory and effector roles during in vivo rejection; our data suggest that the net role of NO is to promote organ rejection. The potential immunoregulatory roles of NO have been demonstrated by discordant reports showing: (*a*) NOS inhibitor-mediated promotion of alloantigen- (12) and mitogen-induced (13) T-lymphocyte proliferation; (*b*) NOS inhibitor-mediated suppression of in vitro T-lymphocyte proliferation (14); and (*c*) NOS inhibitor-mediated promotion of the in vitro proliferation and cytotoxicity of sponge matrix allograft infiltrating cells (15). These reports represent in vitro experiments and thus may not reflect the heterogeneous environment of the in vivo rejection process. The in vitro immunosuppressive action of NO may be explained by the observation that the cytostatic and cytotoxic properties of NO extend to the cells that produce it (29, 30), and thus may also extend to the other cells present in culture, such as lymphocytes.

The significant reduction in cellular infiltrate seen with iNOS inhibition suggests a potential role for NO in the migration of inflammatory cells into the rejecting organ. This is supported by the observation that aminoguanidine reduces the inflammatory cell infiltrate in endotoxin-induced uveitis (10) and in experimental autoimmune encephalomyelitis (11), and by the observation that NO mediates endothelial barrier dysfunction at the site of rejection (Worrall, N. K., K. C. Chang, G. M. Suau, R. G. Tilton, T. P. Misko, J. R. Williamson, and T. B. Ferguson, Jr., manuscript in preparation).

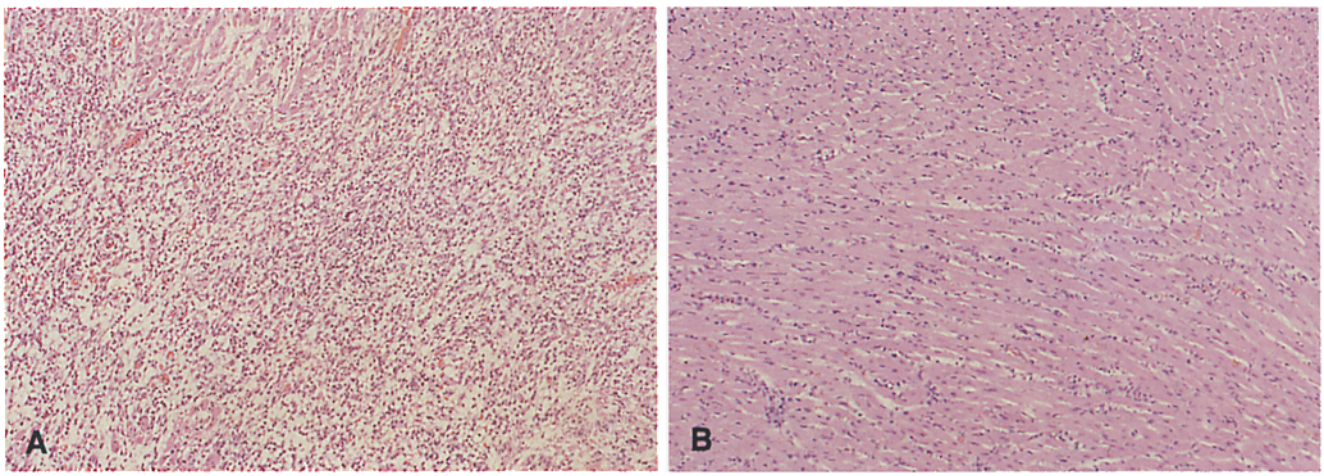

Figure 6. Representative photomicrographs of the subendocardial region of placebo and aminoguanidine-treated allografts hearts harvested on POD-8. (*A*) Placebo-treated allograft demonstrating the severe myocyte necrosis and the dense mononuclear infiltrate characteristic of late rejection. (*B*) Aminoguanidine-treated allograft demonstrating the significant reduction in necrosis and infiltrate with iNOS inhibition. ×50.

The localization of iNOS to the infiltrating cells and the EPR signal for the iron–dinitrosyl complexes are consistent with a cytostatic/cytotoxic effector function of NO, possibly in combination with the generation of oxygen-free radicals. Elucidation of the molecular signals regulating the induction and expression of iNOS in this model may give further insight into the pathogenesis of acute rejection. Inhibition of iNOS may provide a novel therapeutic modality in the management of acute transplant rejection and of other immune-mediated processes.

We are indebted to Drs. Emil Unanue and Thalachallour Mohanakumar for critical review of the manuscript; Dr. Jeffrey Saffitz for guidance in interpreting the histopathology and immunohistochemistry; Dr. Mark G. Currie for thoughtful discussion; Dr. Richard Schuessler for help with the statistical analysis; and to Gloria Suau, Patrick Sullivan, and Darren Alexander for technical assistance.

This work was supported by grants from the National Institutes of Health (1 F32 HL09021-01 to N. K. Worrall and R29 HL46387-03 to T. B. Ferguson, Jr.) and the Monsanto-Searle/Washington University Biomedical Program (to T. B. Ferguson, Jr.).

Address correspondence to Dr. T. Bruce Ferguson, Jr., Division of Cardiothoracic Surgery, Suite 3108 Queeny Tower, One Barnes Hospital Plaza, Saint Louis, MO 63110.

Received for publication 18 July 1994 and in revised form 31 August 1994.

References

1. Lancaster, J.R., Jr., J.M. Langrehr, H.A. Bergonia, N. Murase, R.L. Simmons, and R.A. Hoffman. 1992. EPR detection of heme and nonheme iron-containing protein nitrosylation by nitric oxide during rejection of rat heart allograft. *J. Biol. Chem.* 267:10994–10998.
2. Langrehr, J.M., N. Murase, P.M. Markus, X. Cai, P. Neuhaus, W. Schraut, R.L. Simmons, and R.A. Hoffman. 1992. Nitric oxide production in host-versus-graft and graft-versus-host reactions in the rat. *J. Clin. Invest.* 90:679–683.
3. Moncada, S., R.M.J. Palmer, and E.A. Higgs. 1991. Nitric oxide: physiology, pathophysiology, and pharmacology. *Pharmacol. Rev.* 43:109–142.
4. Nathan, C. 1992. Nitric oxide as a secretory product of mammalian cells. *FASEB (Fed. Am. Soc. Exp. Biol.) J.* 6:3051–3064.
5. Hibbs, J.B., Jr., R.R. Taintor, Z. Vavrin, D.L. Granger, J.-C. Drapier, I.J. Amber, and J.R. Lancaster, Jr. 1990. Synthesis of nitric oxide from a terminal guanidino nitrogen atom of L-arginine: a molecular mechanism regulating cellular proliferation that targets intracellular iron. *In* Nitric Oxide from L-Arginine: A Bioregulatory System. S. Moncada and E.A. Higgs, editors. Elsevier, Amsterdam. 189–223.
6. Stuehr, D.J., and C.F. Nathan. 1989. Nitric oxide: a macrophage product responsible for cytostasis and respiratory inhibition in tumor target cells. *J. Exp. Med.* 169:1543–1555.
7. Misko, T.P., W.M. Moore, T.P. Kasten, G.A. Nickols, J.A. Corbett, R.G. Tilton, M.L. McDaniel, J.R. Williamson, and M.G. Currie. 1993. Selective inhibition of the inducible nitric oxide synthase by aminoguanidine. *Eur. J. Pharmacol.* 233: 119–125.
8. Tilton, R.G., K. Chang, K.S. Hasan, S.R. Smith, J.M. Petrash, T.P. Misko, W.M. Moore, M.G. Currie, J.A. Corbett, M.L. McDaniel, and J.R. Williamson. 1993. Prevention of diabetic vascular dysfunction by guanidines. Inhibition of nitric oxide synthase versus advanced glycation end-product formation. *Diabetes.* 42:221–232.
9. Corbett, J.A., A. Mikhael, J. Shimizu, K. Frederick, T.P. Misko, M.L. McDaniel, O. Kanagawa, and E.R. Unanue. 1993. Nitric oxide production in islets from nonobese diabetic mice: aminoguanidine-sensitive and -resistant stages in the immunological diabetic process. *Proc. Natl. Acad. Sci. USA.* 90:8992–8995.
10. Tilton, R.G., K. Chang, J.A. Corbett, T.P. Misko, M.G. Currie, N.S. Bora, H.J. Kaplan, and J.R. Williamson. 1994. Endotoxin-induced uveitis in the rat is attenuated by inhibition of nitric oxide production. *Invest. Ophthalmol. & Visual Sci.* 35:3278–3288.
11. Cross, A.H., T.P. Misko, R.F. Lin, W.F. Hickey, J.L. Trotter, and R.G. Tilton. 1994. Aminoguanidine, an inhibitor of inducible nitric oxide synthase, ameliorates experimental autoimmune encephalomyelitis in SJL mice. *J. Clin. Invest.* 93:2684–2690.
12. Hoffman, R.A., J.M. Langrehr, T.R. Billiar, R.D. Curran, and R.L. Simmons. 1990. Alloantigen-induced activation of rat splenocytes is regulated by the oxidative metabolism of L-arginine. *J. Immunol.* 145:2220–2226.
13. Mills, C.D. 1991. Molecular basis of "suppressor" macrophages. Arginine metabolism via the nitric oxide synthetase pathway. *J. Immunol.* 146:2719–2723.
14. Gregory, S.H., A.J. Sagnimeni, and E.J. Wing. 1994. Arginine analogues suppress antigen-specific and -nonspecific T lymphocyte proliferation. *Cell. Immunol.* 153:527–532.
15. Langrehr, J.M., K.E. Dull, J.B. Ochoa, T.R. Billiar, S.T. Ildstad, W.H. Schraut, R.L. Simmons, and R.A. Hoffman. 1992. Evidence that nitric oxide production by in vivo allosensitized cells inhibits the development of allospecific CTL. *Transplantation (Baltimore).* 53:632–640.
16. Ono, K., and E.S. Lindsey. 1969. Improved technique of heart transplantation in rats. *J. Thorac. Cardiovasc. Surg.* 57:225–229.
17. Misko, T.P., R.J. Schilling, D. Salvemini, W.M. Moore, and M.G. Currie. 1993. A fluorometric assay for the measurement of nitrite in biological samples. *Anal. Biochem.* 214:11–16.
18. Chomczynski, P., and N. Sacchi. 1987. Single-step method of RNA isolation by acid guanidinium thiocyanate-phenol-chloroform extraction. *Anal. Biochem.* 162:156–159.

19. Bredt, D.S., and S.H. Snyder. 1990. Isolation of nitric oxide synthethase, a calmodulin-requiring enzyme. *Proc. Natl. Acad. Sci. USA.* 87:682–685.
20. Finkel, M.S., C.V. Oddis, T.D. Jacob, S.C. Watkins, B.G. Hattler, and R.L. Simmons. 1992. Negative inotropic effects of cytokines on the heart mediated by nitric oxide. *Science (Wash. DC).* 257:387–389.
21. Billingham, M.E. 1981. Diagnosis of cardiac rejection by endomyocardial biopsy. *Heart Transplantation.* 1:25–30.
22. Imagawa, D.K., J.M. Millis, P. Seu, K.M. Olthoff, J. Hart, E. Wasef, R.A. Dempsey, S. Stephens, and R.W. Busuttil. 1991. The role of tumor necrosis factor in allograft rejection: III. Evidence that anti-TNF antibody therapy prolongs allograft survival in rats with acute rejection. *Transplantation (Baltimore).* 51:57–62.
23. Balligand, J.-L., D. Ungureanu, R.A. Kelly, L. Kobzik, D. Pimental, T. Michel, and T.W. Smith. 1993. Abnormal contractile function due to induction of nitric oxide synthesis in rat cardiac myocytes follows exposure to activated macrophage-conditioned medium. *J. Clin. Invest.* 91:2314–2319.
24. Henry, Y., C. Ducrocq, J.-C. Drapier, D. Servent, C. Pellat, and A. Guissani. 1991. Nitric oxide, a biological effector. *Eur. Biophys. J.* 20:1–15.
25. Stadler, J., H.A. Bergonia, M. Di Silvio, M.A. Sweetland, T.R. Billiar, R.L. Simmons, and J.R. Lancaster, Jr. 1993. Nonheme iron-nitrosyl complex formation in rat hepatocytes: detection by electron paramagnetic resonance spectroscopy. *Arch. Biochem. Biophys.* 302:4–11.
26. Lancaster, J.R., Jr., and J.B. Hibbs, Jr. 1990. EPR demonstration of iron-nitrosyl complex formation by cytotoxic activated macrophages. *Proc. Natl. Acad. Sci. USA.* 87:1223–1227.
27. Zweier, J.L., J.T. Flaherty, and M.L. Weisfeldt. 1987. Direct measurement of free radical generation following reperfusion of ischemic myocardium. *Proc. Natl. Acad. Sci. USA.* 84: 1404–1407.
28. Beckman, J.S., T.W. Beckman, J. Chen, P.A. Marshall, and B.A. Freeman. 1990. Apparent hydroxyl radical production by peroxynitrite: implications for endothelial injury from nitric oxide and superoxide. *Proc. Natl. Acad. Sci. USA.* 87:1620–1624.
29. Drapier, J.-C., and J.B. Hibbs, Jr. 1988. Differentiation of murine macrophages to express nonspecific cytotoxicity for tumor cells results in L-arginine dependent inhibition of mitochondrial iron-sulfur enzymes in the macrophage effector cells. *J. Immunol.* 140:2829–2838.
30. Albina, J.E., M.D. Caldwell, W.L. Henry, Jr., and C.D. Mills. 1989. Regulation of macrophage functions by L-arginine. *J. Exp. Med.* 169:1021–1029.